Effects of photoionization on similarity properties of streamers at various pressures in air

N Liu and V P Pasko

Communications and Space Sciences Laboratory, Department of Electrical Engineering,
Pennsylvania State University, University Park, PA 16802, USA

E-mail: nul105@psu.edu and vpasko@psu.edu

Abstract
Modelling studies are presented of positive streamers developing at various
pressures in air in a point-to-plane discharge geometry. The modelling
results emphasize that the quenching of the singlet excited states of
molecular nitrogen emitting photoionizing radiation is responsible for
non-similar behaviour of streamers at pressures higher than approximately
30 Torr. Our modelling results are consistent with recent experimental work
showing that streamers have more and thinner channels and branch more
frequently at higher (i.e. near atmospheric) pressures than at lower pressures.
The results also demonstrate the importance of accounting for effects
associated with electrode geometry for the interpretation of experimental
studies on similarity properties of streamers at various pressures.

1. Introduction

About a decade ago large-scale electrical discharges
were discovered in the Earth's atmosphere above large
thunderstorms, which are now commonly referred to as sprites
[1]. Telescopic imaging of sprites has revealed an amazing
variety of decametre-scale filamentary structures in these
events [2]. Surprisingly, the filamentary structures observed in
sprites are the same phenomenon known as streamer discharges
at atmospheric pressure, only scaled by reduced air density
at higher altitudes [3–5]. Streamers are narrow filamentary
plasmas, which are driven by highly nonlinear space charge
waves [6, p 317]. Streamer discharges are commonly used
to generate chemically active species to remove pollutants in
various gases [7] and also represent important components
involved in the triggering of combustion in spark ignition
engines [8, 9]. Lightning is another natural phenomenon
related to streamer discharges. A streamer zone consisting
of many highly-branched streamers usually precedes leader
channels initiating lightning discharges in large volumes at
near ground pressure [6, p 364].

Streamer discharges represent an example of a highly
nonlinear and self-consistent phenomenon, which is not fully
understood at present. Streamers are commonly observed with
branching structures; however, experimental and theoretical
work on understanding of the branching mechanism of
streamers is still in the preliminary stage. Using a minimal
streamer model accounting for the transport and impact
ionization processes of electrons in non-attaching gas such as
argon and nitrogen, Arrayás *et al* [10] numerically simulated a
negative streamer propagating between two planar electrodes
in a uniform external electric field with a very large magnitude.
It was demonstrated that the streamers, in cases when no
preionization is available ahead of them, reach an unstable
'ideal conductivity' state with an approximately equipotential
and weakly curved head. It was proposed that this new
state exhibits a Laplacian instability, like that in viscous
fingering, which leads to the branching of the streamer [10].
Recent research work directed on understanding the role of
photoionization processes in the development of streamer
discharges indicates that the photoionization is a critical factor
defining the branching conditions of streamers [4, 11–13].
Modelling results [4] show that the photoionization acts as
a physical mechanism to adjust the ratio of the electric field
in the streamer head to the electric field in the streamer
channel. The expansion of streamers in strong applied electric

fields leads to an increase of this ratio and the streamer splits after reaching a state with a weakly curved and equipotential head similar to that discussed by Arrayás *et al* [10]. The branching of streamers is a complex phenomenon which, in real systems, depends also on the external circuit parameters and the configuration of electrodes [14].

In weakly ionized plasma physics, similarity relations [15, p 306] are well-recognized to identify the parameters of gas discharge plasmas at different pressures. Similarity relations represent a useful tool in the analysis of gas discharges since they allow us to use known properties of the discharge at one pressure to deduce features of discharges at various of other pressures of interest, at which experimental studies may not be feasible or even possible. If an electron is placed in a uniform electric field E between two electrodes with a gap size d, the increase in energy of the electron is a function of the product $E\lambda$, where λ is the mean free path that is inversely proportional to the gas number density N or pressure p. We note that in this paper we use neutral density N in place of pressure p and vice versa, therefore assuming a constant (room) temperature of ambient neutral gas. It is expected that similar discharges can be obtained if the product $E\lambda$ and the mean free path number d/λ are kept constant ([16] and references cited therein). In other words, to be able to compare discharges at different pressures p the scaling factors E/p and pd must be kept constant [16]. Similarity laws for streamers propagating in non-uniform gaps in air at high (i.e. several atmospheric) pressures have been studied in previous research work [8, 16]. The observed deviations from similarity at high pressures in experiments reported in [8, 16] have been attributed by the authors to gas heating effects leading to the formation of a hot channel due to the streamer-to-leader transition. The similarity properties of streamers at different air pressures are also of great interest for the interpretation of morphology observed in high altitude sprite discharges [3, 4]. In accordance with the similarity laws, the streamer timescales, the streamer spatial scales and the streamer electron density scale with the air density as $\sim 1/N$, $\sim 1/N$ and $\sim N^2$, respectively, and the scaled streamer characteristics remain otherwise identical for the same values of the reduced electric field E/N. When the photoionization effects are not taken into account, the above-listed set of similarity relations works very well for describing characteristics of short streamers (i.e. when three-body attachment, recombination, gas heating and thermal conduction processes are negligible) at near and lower than atmospheric pressures. When the photoionization effects are included, streamers at pressures lower than several Torr preserve similarity, but similarity laws do not hold at higher pressures [4]. These predictions appear to be consistent with the recent experimental studies of similarity properties of positive streamers at different pressures in air [17, 18].

Our previous work [4] has demonstrated that the photoionization process is the most critical factor contributing to non-similar behaviour of streamers propagating in strong homogeneous external electric fields ($> E_k$, where E_k is the conventional breakdown threshold field defined by the equality of the ionization and dissociative attachment coefficients in air [6, p 135]). In this paper, we present modelling results on the dynamics of streamers at various pressures developing in a point-to-plane discharge geometry, which are directly relevant to the interpretation of recent experiments [17, 18].

2. Model formulation

To study the dynamics of streamers, the most common and effective model is the hydrodynamic description of motion of charged particles driven by the superposition of their own space charge and external electric fields. The model used for studies reported in this paper includes the electron and ion drift–diffusion equations coupled with Poisson's equation:

$$\frac{\partial n_e}{\partial t} + \nabla \cdot n_e \vec{v}_e - D_e \nabla^2 n_e = (\nu_i - \nu_{a2} - \nu_{a3})n_e$$
$$- \beta_{ep} n_e n_p + S_{ph}, \tag{1}$$

$$\frac{\partial n_p}{\partial t} = \nu_i n_e - \beta_{ep} n_e n_p - \beta_{np} n_n n_p + S_{ph}, \tag{2}$$

$$\frac{\partial n_n}{\partial t} = (\nu_{a2} + \nu_{a3})n_e - \beta_{np} n_n n_p, \tag{3}$$

$$\nabla^2 \Phi = -\frac{e}{\epsilon_0}(n_p - n_e - n_n), \tag{4}$$

where n_e, n_p and n_n are the electron, positive-ion and negative-ion number densities, respectively, $\vec{v}_e$ is the drift velocity of electrons, ν_i is the ionization frequency, ν_{a2} and ν_{a3} are the two-body and three-body electron attachment frequencies, respectively, β_{ep} and β_{np} are the coefficients of electron-positive ion and negative-positive ion recombination, respectively, D_e is the electron diffusion coefficient, S_{ph} is the rate of electron–ion pair production due to photoionization, Φ is the electric potential, e is the absolute value of electron charge and ε_0 is the permittivity of free space. The electron drift velocity is defined as $\vec{v}_e = -\mu_e \vec{E}$, where μ_e is the absolute value of the electron mobility and $\vec{E} = -\nabla\Phi$ is the electric field. On timescales of interest for studies presented in this paper, the ions are assumed to be motionless. This assumption is fully justified by the fact that the mobilities of positive and negative ions are two orders of magnitude lower than the electron mobility [11]. The model accounts for the photoionization effects on the streamer dynamics using a physical model proposed in [19]. A detailed description of the sources of constants and rate coefficients utilized in this study can be found in [4, 20].

The geometry of the simulation domain is illustrated in figure 1, which is identical to that proposed in [21] for studies of the dynamics of streamers in weak uniform electric fields. The technique that we use to obtain the solution of the electric field in this system is the same as that described by Babaeva and Naidis [21]. The solution for the electric potential can be represented in the following form [22]:

$$\Phi(\vec{r}) = \Phi_L(\vec{r}) + \frac{1}{4\pi\varepsilon_0} \iiint_{V'} \frac{\rho_Q(\vec{r}')}{|\vec{r} - \vec{r}'|} dV', \tag{5}$$

where Φ_L corresponds to the ambient Laplacian field established by two remote plane electrodes and a conducting sphere charged to potential Φ_0 (see figure 1), $\rho_Q(\vec{r}') = e(n_p - n_e - n_n)$ is the free charge density at the source point $\vec{r}'$ and $\vec{r}$ is the observation point. The integral is taken over the volume containing space charges and their images in the conducting sphere. Solution (5) is used to calculate the electric potential at the boundary of the simulation domain only. Inside the domain, the values of Φ are computed by the successive over-relaxation (SOR) method [23, p 179]. In the cylindrical system of coordinates specified in figures 1 and 2 and assuming that
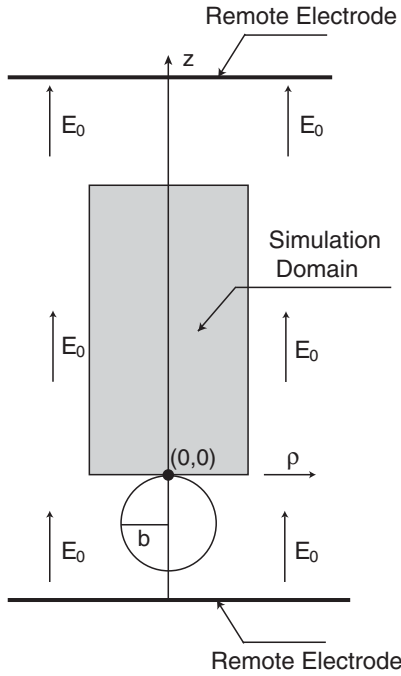
Figure 1. Simulation domain. A potential Φ_0 is applied to the conducting sphere with radius b which is put into an originally homogeneous field E_0 established by two remote plane electrodes.
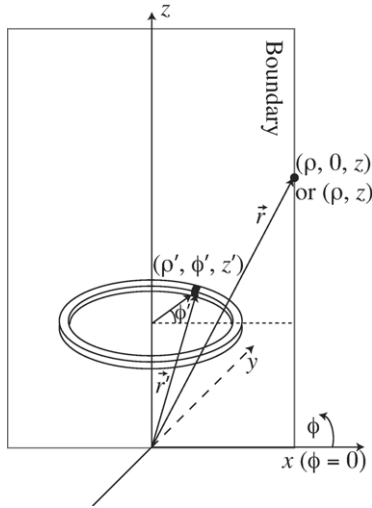

Figure 2. Charge integration geometry.

the conducting sphere is charged to potential Φ_0 the Laplacian potential Φ_L is represented in the form:

$$\Phi_L(\rho, z) = \Phi_0 \left(\frac{b}{r_s}\right) - E_0 \left[1 - \left(\frac{b}{r_s}\right)^3\right](z+b), \quad (6)$$

where $r_s = \sqrt{(b+z)^2 + \rho^2}$ is the distance between the sphere centre and the observation point (ρ, z).

By calculating the potential contribution at the boundary due to charges $\rho_Q(\vec{r})$, we account for the space charges in the computational domain and their images due to the presence of the conducting sphere. The streamer model is cylindrically symmetric, and the space charge inside the computational domain can be represented by many homogeneously charged

rings with a small cross section, corresponding to the individual grid points in (ρ, z) domain and centred at the axis of the symmetry (figure 2). Using the cylindrical coordinate system, the electric potential $d\Phi(\rho, z)$ at boundary position (ρ, z) (see figure 2) caused by an elemental ring is

$$d\Phi(\rho, z) = \frac{1}{4\pi\varepsilon_0} \rho_Q(\rho', z')\rho' d\rho' dz'$$
$$\times \int_0^{2\pi} \frac{1}{\sqrt{\rho^2 - 2\rho\rho'\cos\phi' + \rho'^2 + (z-z')^2}} d\phi'. \quad (7)$$

Having substituted $\phi' = \pi + 2\beta$ in equation (7), after straightforward algebraic manipulations this equation can be written in the form:

$$d\Phi(\rho, z) = \frac{1}{4\pi\varepsilon_0} \frac{\left[\rho_Q(\rho', z')2\pi\rho' d\rho' dz'\right]}{\sqrt{(\rho+\rho')^2 + (z-z')^2}} \frac{4\mathcal{K}(k)}{2\pi}, \quad (8)$$

where the term in the square brackets is the amount of charge in an elemental ring, $k^2 = 4\rho\rho'/[(\rho+\rho')^2 + (z-z')^2]$, and $\mathcal{K}(k) = \int_0^{\pi/2}(1 - k^2 \sin^2\beta)^{-1/2} d\beta$ is the complete elliptic integral of the first kind (an efficient algorithm to calculate $\mathcal{K}(k)$ is readily available [24, p 267]).

For the source charges corresponding to grids on the axis of symmetry equation (8) is represented in the form:

$$d\Phi(\rho, z) = \frac{1}{4\pi\varepsilon_0} \frac{[\rho_Q(\rho', z')\pi(d\rho'/2)^2 dz']}{\sqrt{\rho^2 + (z-z')^2}}, \quad (9)$$

where $4\mathcal{K}(0)/2\pi = 1$ is applied.

The total contribution of the source charges inside the simulation domain to the potential values at the boundary can be obtained by a simple summation of differential contributions, corresponding to individual grid points, given by equations (8) and (9).

The source charges inside the simulation domain also generate image charges in the conducting sphere and contributions of these charges to the potential values at the boundary can be evaluated as follows. For the source charge Q shown in figure 3(a), the image charge Q_i and its location d_i are $Q_i = -(b/d)Q$ and $d_i = (b^2/d)$ [25, p 147]. For the geometry shown in figure 3(b), we have $d = \sqrt{\rho^2 + z^2}$, so that $Q_i = -(b/d)Q$, $\rho_i = (b^2/d^2)\rho$ and $z_i = (b^2/d^2)z$. For the coordinate system used in our studies, which is shown by figures 1 and 3(c), the set of equations for the image charge is transformed into $d = \sqrt{(b+z)^2 + \rho^2}$, $Q_i = -(b/d)Q$, $\rho_i = (b^2/d^2)\rho$ and $z_i = (b^2/d^2)(z+b) - b$.

The total summation corresponding to the integral in the last term of equation (5) accounting for charges inside the simulation domain and their images can therefore be represented in the form:

$$\iiint_{V'} \frac{\rho_Q(\vec{r}')}{|\vec{r} - \vec{r}'|} dV' = \iint \frac{d\rho' dz' 2\pi\rho' \rho_Q(\rho', z')}{\sqrt{(\rho+\rho')^2 + (z-z')^2}} \frac{4\mathcal{K}(k)}{2\pi}$$
$$- \iint \frac{d\rho' dz'(b/d)2\pi\rho' \rho_Q(\rho', z')}{\sqrt{(\rho+\rho_i')^2 + (z-z_i')^2}} \frac{4\mathcal{K}(k_i)}{2\pi}, \quad (10)$$

where $\rho_i' = (b^2/d^2)\rho'$, $z_i' = [(b^2/d^2)(z'+b) - b]$, $d = \sqrt{(b+z')^2 + \rho'^2}$ and $k_i^2 = 4\rho\rho_i'/[(\rho+\rho_i')^2 + (z-z_i')^2]$. Similar expressions can be generated to account for contributions of source charges corresponding to grids on the axis of symmetry.

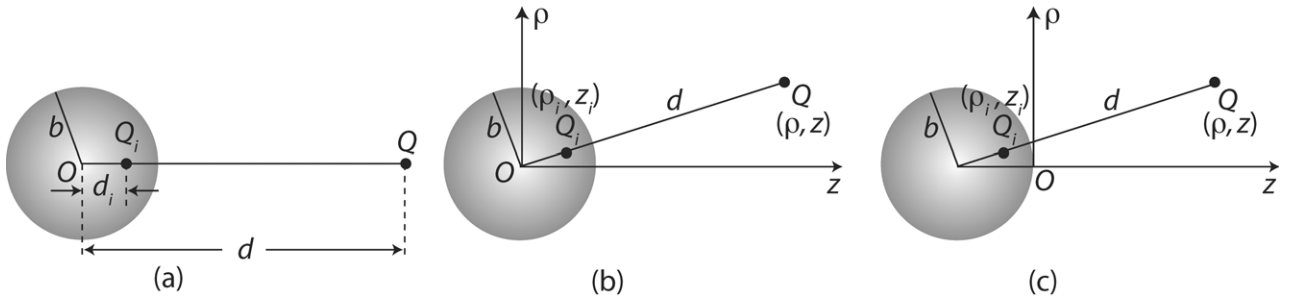**Figure 3.** Geometry for calculating the point charge and its image for a conducting sphere.
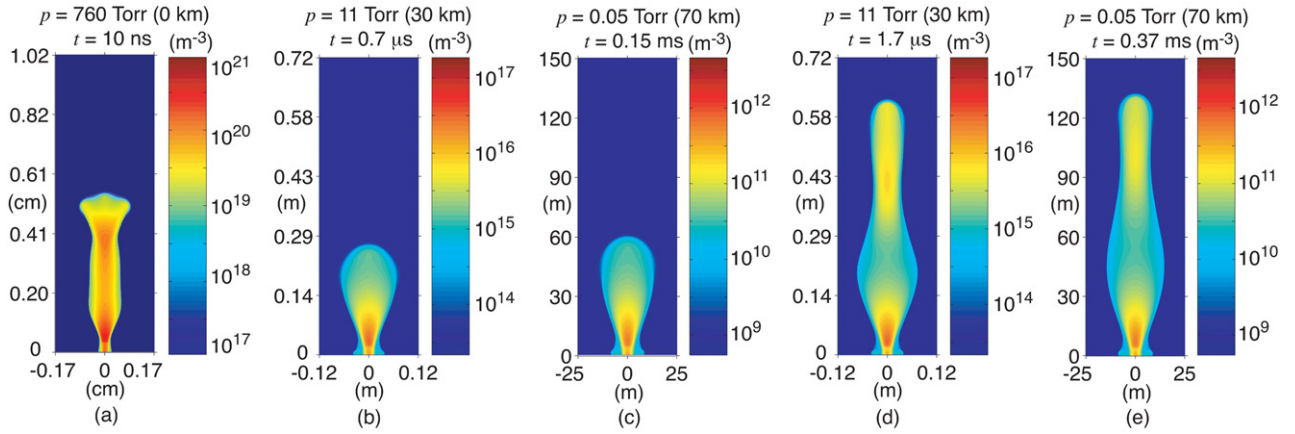

Figure 4. A cross-sectional view of the distribution of the electron number density for a positive streamer developing at different pressures in a field $E_0 = 5N/N_0 \, \text{kV cm}^{-1}$, and assuming spherical electrode potential $\Phi_0 = 9.5 \, \text{kV}$. Panels (*a*), (*b*) and (*c*) correspond to streamers at moments of time $10 \, N_0/N$ ns. Panels (*d*) and (*e*) show fully-developed streamers corresponding to panels (*b*) and (*c*), respectively.

When considering the similarity relations of streamers at various pressures, it is necessary to make sure that streamers develop under the influence of the same reduced external electric fields. For the first set of results presented in the next section we keep $E_0 N_0/N$ constant for all the studied pressures, where N and N_0 are neutral densities at the pressure of interest and at the ground level, respectively. For example, $E_0 = 5 N/N_0 \, \text{kV cm}^{-1}$ corresponds to $E_0 = 5 \, \text{kV cm}^{-1}$ at 760 Torr and $2.5 \, \text{kV cm}^{-1}$ at 380 Torr. Additionally, we keep the potential applied to the spherical electrode Φ_0 constant and vary its radius b and the size of the simulation domain (see figure 1) proportionally to N_0/N (in other words, we keep bN/N_0 constant following the similarity laws for non-uniform gaps discussed in [8, 16]). For the initiation of streamers propagating at different pressures, we place a cloud of plasma with peak density $10^{18} N^2/N_0^2 \, \text{m}^{-3}$ and the spherically symmetric Gaussian spatial distributions with characteristic scale $10^{-4} N_0/N$ m on the axis of symmetry in the vicinity of the sphere, which is assumed to have radius $b = 10^{-3} N_0/N$ m.

3. Results and discussion

Figure 4 shows results of model calculations corresponding to positive streamers developing at different pressures assuming $E_0 = 5N/N_0 \, \text{kV cm}^{-1}$ and $\Phi_0 = 9.5 \, \text{kV}$. To clearly demonstrate similarity properties of streamers at different pressures, the results presented in figures 4(*b*) and (*c*) are

given at the moments of time, which are obtained by scaling ($\sim 1/N$) of the ground value, 10 ns, specified in figure 4(*a*). It follows from the results presented in figures 4(*b*)–(*e*) that streamers at 11 and 0.05 Torr pressures preserve similarity and propagate without branching, while a model streamer at 760 Torr (figure 4(*a*)) shows branching structures. The streamers at low pressures initially quickly expand and then evolve into a stable propagation stage with a constant radius. The explanation of this behaviour is based on the spatial distribution of the external field: the enhancement of the field near the sphere gradually fades away and the magnitude of the field approaches E_0 at a distance $4b$ from the sphere [26]. Therefore, the streamer expands in the high field region and then propagates with a constant radius in E_0, which for results presented in figure 4 is also close to the stability field (see additional discussion on expansion of streamers in [4, 26]). The ground level streamer (figure 4(*a*)) shows no branching structures by 6.5 ns and propagates with a speed about $6 \times 10^5 \, \text{m s}^{-1}$, which is substantially higher than velocities ($\sim 3.6 \times 10^5 \, \text{m s}^{-1}$) of well-developed streamers at 11 and 0.05 Torr shown in figures 4(*d*) and (*e*). During this stage, the ground level streamer exhibits substantially higher electric field values in its head, which is consistent with similar results reported in [4]. The streamer at 760 Torr is also narrower and its electron density is higher than the scaled streamers at low pressures (i.e. obtained by the multiplication of their radius by N/N_0 and density by N_0^2/N^2). These results agree with the conclusion drawn in [4] that the quenching of the excited singlet states of N_2, emitting photoionizing
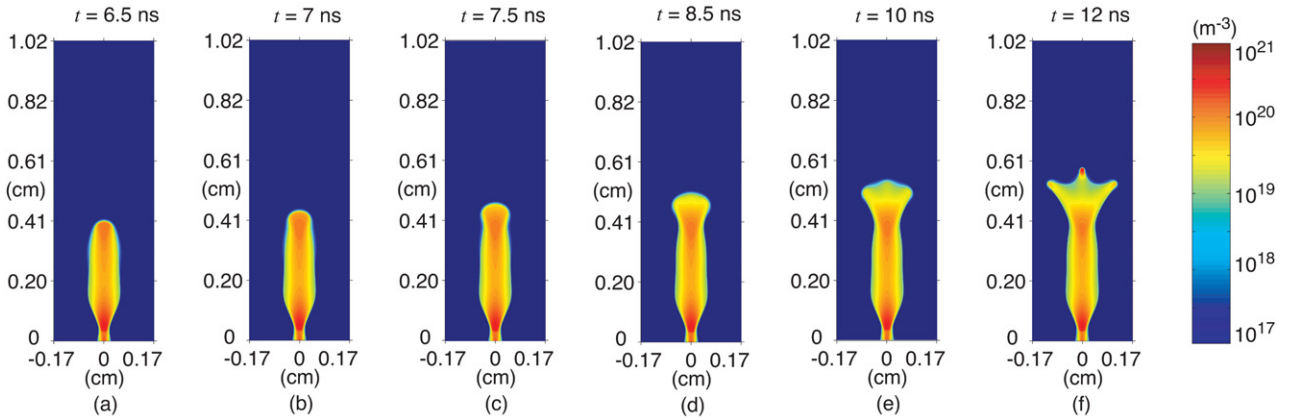
Figure 5. A cross-sectional view of the distribution of the electron number density for the ground level streamer shown in figure 4(a) at a sequence of moments of time: 6.5 ns (a), 7 ns (b), 7.5 ns (c), 8.5 ns (d), 10 ns (e) and 12 ns (f).

Figure 6. A cross-sectional view of the distribution of the electric field for the ground level streamer shown in figure 4(a) at a sequence of moments of time: 6.5 ns (a), 7 ns (b), 7.5 ns (c), 8.5 ns (d), 10 ns (e) and 12 ns (f).
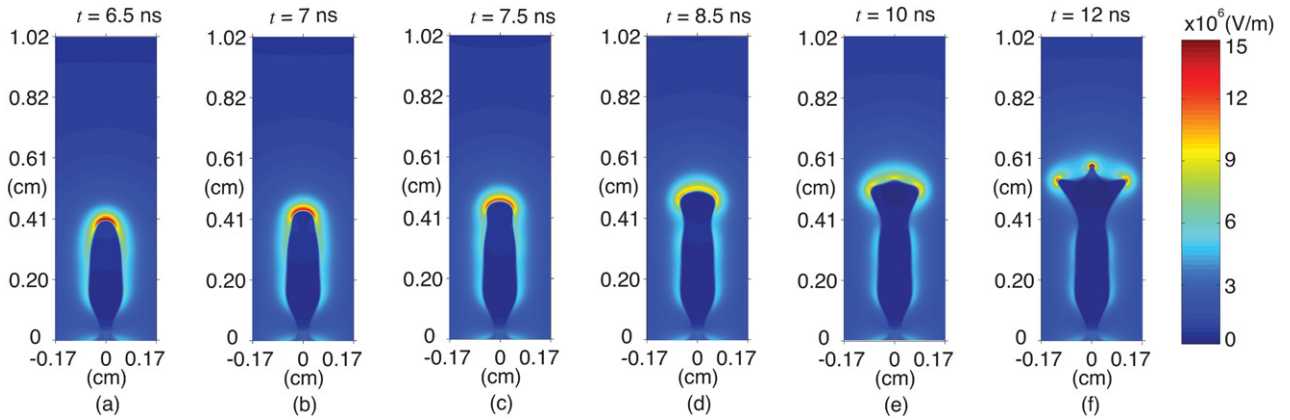
radiation, is responsible for non-similar behaviour of streamers at high pressures (i.e. the streamer in figure 4(a)). The quenching altitude of the above mentioned singlet states is ~24 km (corresponding to 30 Torr pressure). Therefore the quenching effects are negligible at low pressures $p < 30$ Torr corresponding to altitudes >24 km, and streamers at 11 and 0.05 Torr pressures preserve similarity (figures 4(b) and (c)). At ground pressure, the excited singlet states are heavily quenched, and the photoionizing radiation level is reduced by a factor of ~20 in comparison with cases of streamers at 11 and 0.05 Torr pressures (see [4] for additional discussion on related issues).

Figures 5 and 6 show the distributions of the electron number density and the electric field for the ground level streamer (figure 4(a)) at a sequence of moments of time after 6.5 ns. The location of the maximum field of the streamer is on the z axis before 6.5 ns, and this point gradually deviates from the z axis after the streamer starts to branch. The propagation speed of the streamer in the z direction is sharply reduced to 1.8×10^5 m s^{-1} in 3.5 ns.

To further visualize similarities and differences of streamers at different pressures, we plot the streamer length as a function of time and the maximum field on the axis of symmetry in figures 7(a) and (b), respectively, where the plotted values are obtained after proper scaling of the original simulation results, i.e. time and length are multiplied by N/N_0

and field by N_0/N. These two figures clearly show that the streamer length and the maximum field vary in agreement with similarity relations for low pressure cases ($p = 11$ Torr and $p = 0.05$ Torr), while the characteristics of the streamer at $p = 760$ Torr significantly deviate from those expected from similarity relations. In particular, figure 7(a) demonstrates that the speed of the streamer at $p = 760$ Torr is greater than that at low pressures; figure 7(b) demonstrates that the maximum field of the streamer at $p = 760$ Torr is greater than that at low pressures, as we have discussed previously. It is also noted that both the speed and the maximum field of the streamer at $p = 760$ Torr sharply decrease right after the branching.

In [4], we have proposed a physical mechanism for the streamer branching indicating that streamers are easier to branch at ground level due to the reduction of preionization level ahead of the streamer due to quenching of the N_2 states emitting photoionizing radiation. The results presented in figure 4 are consistent with this branching mechanism. We have proposed a relationship defining the streamer radius ($r_{s\,max}$) preceding the branching, $r_{s\,max} \simeq \kappa/\chi_{min} p_{O_2}$, where κ is a dimensionless parameter, χ_{min} is the absorption cross-section of O_2 at wavelength 102.5 nm and p_{O_2} is the partial pressure of O_2. It was suggested that the value of κ varies with pressure and that we generally expect lower values of κ and smaller splitting diameters of streamers at the ground level in comparison with sprite altitudes due to the quenching
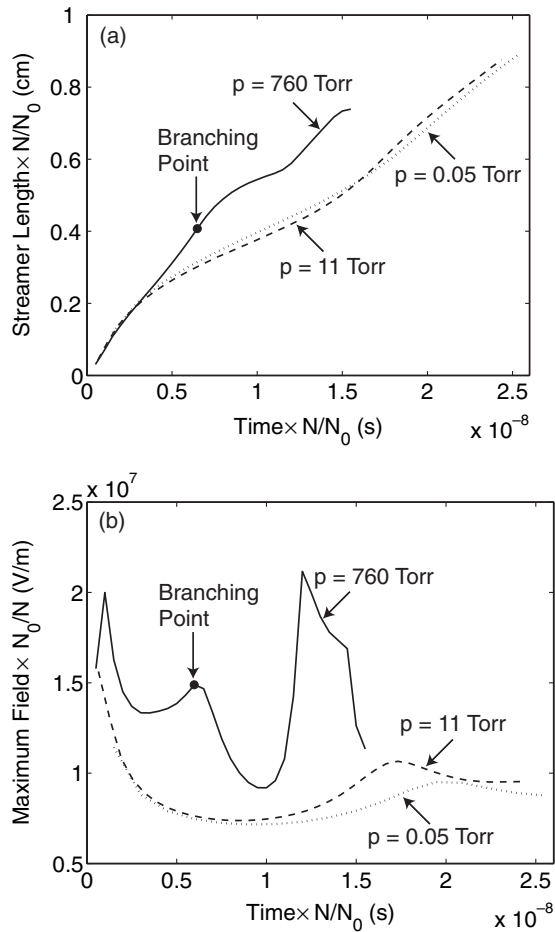
Figure 7. (*a*) Streamer length as a function of time. The streamer length is defined as the distance between the origin and the location of the maximum field on the axis of symmetry. (*b*) The maximum field on the axis of symmetry as a function of time. In both (*a*) and (*b*), solid lines are for $p = 760$ Torr, dashed lines for $p = 11$ Torr and dotted lines for $p = 0.05$ Torr. The plotted values are obtained after proper scaling of the original simulation results, i.e. time and length are multiplied by N/N_0 and field by N_0/N.

effects [4]. The results shown by figure 4 clearly verify this prediction.

We now discuss our modelling results in the context of recently published experimental work on the development of positive streamers at different pressures.

Results of the experimental investigation of positive streamer discharges in air for the pressure range from 760 to 300 Torr are reported in [17]. The streamers propagated in a gap with the same size $d = 30$ mm and were driven by the external electric field of the same magnitude $E_{gap} = 7$ kV cm^{-1} for all studied pressures. The streamers initiated from a needle anode and propagated towards a plane cathode. The time-integrated photographs clearly show that streamers exhibit many branches several branches and a single channel at pressures of 740 Torr, 500 Torr and 380 Torr, respectively [17]. In terms of discussion of similarity properties of streamers presented earlier in this paper the experimental setup used in [17] corresponds to a factor of two increase in the reduced electric field E/N and a factor of two decrease in the effective gap size and radius of the anode (the effective gap size, for example, is defined as dN/N_0), when pressure is changed

from 740 to 380 Torr. For accurate studies of the streamer similarity, however, it is desirable to keep the same reduced electric field and scale the gap and the point-electrode size as N_0/N (in other words, to keep the effective gap size dN/N_0 constant). In this particular experiment, therefore, factors which contribute to the observed non-similar behaviour of streamers at different pressures include (1) different reduced field magnitudes, (2) different effective gap size and anode radius and (3) the pressure defined quenching effects discussed earlier in this paper. However, figure 3 in [17] demonstrates that the maximum diameter of the observed streamers does not scale as N_0/N, suggesting that κ varies with pressure and exhibits lower values at higher pressures. This finding is consistent with the behaviour predicted in [4] based on the fact that branching diameters of streamers are expected to increase with reduction of pressure due to reduction in quenching losses of excited N_2 molecules responsible for photoionizing radiation, as illustrated in the first part of this paper. We emphasize, however, that different reduced electric fields, effective gap sizes and anode radii used in [17] do not allow direct quantitative verification of the quenching-based hypothesis advanced in [4].

Experimental studies of propagation and branching of positive streamers in air in a pressure ranging from 1010 to 100 mbar have been recently reported in [18]. The experiments were conducted in a 17 mm gap consisting of a point anode and plane cathode, with adjustable anode voltage. The obtained time integrated ($10 \mu s$) pictures of streamers demonstrate that streamer discharges have more and thinner channels at high pressures than at low pressures. By imaging streamers developing under conditions of different applied voltages (U) and pressures (p), the authors clearly established that streamer branching structures are not simply determined by U/p (or E/N). For the same values of U/p, streamers have more channels at high pressures than at low pressures. These findings are generally consistent with our modelling results presented in figure 4 and in [4] indicating that quenching effects facilitate easier branching of streamers at high pressures than at low pressures. We note, however, that following the same arguments as presented above with relation to experiments in [17], the constant gap size and radius of point anode in experiments reported in [18] represent additional factors affecting observed non-similar behaviour of streamers at different pressures (additional comments on this issue will be provided below).

To further illustrate the above discussed points, we present our model results for two selected cases closely resembling the combination of parameters of experiments reported in [17] and [18]. We use exactly the same electrode geometry as was used to obtain results shown in figure 4(*a*) and keep the gap size (1.02 cm) and the spherical electrode radius ($b = 1$ mm) unchanged. Figures 8(*a*) and (*b*) show streamers developing in air at 380 Torr pressure in a simulation domain having the same size in the z direction as in figure 4(*a*), while the size of the simulation domain in the radial direction is adjusted in figure 8(*a*) to allow enough room for the free radial development of the streamer.

For the case shown in figure 8(*a*) we assume $E_0 = 5$ kV cm^{-1} and $\Phi_0 = 9.5$ kV. The reduced external field in this case is two times larger than that in figure 4(*a*) similarly
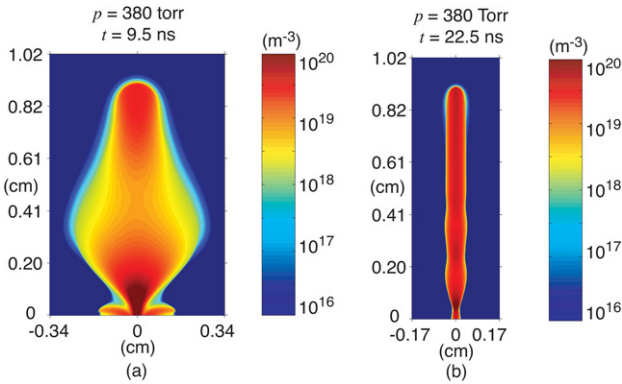
Figure 8. A cross-sectional view of the distribution of the electron number density for a model positive streamer under the following conditions: (a) $E_0 = 5 \, \text{kV cm}^{-1}$, $\Phi_0 = 9.5 \, \text{kV}$ and $p = 380 \, \text{Torr}$; (b) $E_0 = 5N/N_0 \, \text{kV cm}^{-1}$, $\Phi_0 = 9.5N/N_0 \, \text{kV}$ and $p = 380 \, \text{Torr}$.

to the conditions of experiments presented in [17]. Initially the peak field at the surface of the spherical electrode is about $8E_k$. This extremely large field produces intense ionization creating a bulk of plasma around the sphere, and the streamer is formed from this plasma cloud. It appears that the streamer just starts to propagate before it reaches the upper boundary of the simulation domain. The fast initial expansion of ionization in figure 3(a) is consistent with the streamer structure reported for 380 Torr pressure in figure 2 of [17].

Figure 8(b) shows the development of a streamer in the same gap but assuming $E_0 = 5N/N_0 \, \text{kV cm}^{-1}$ and $\Phi_0 = 9.5N/N_0 \, \text{kV}$. The conditions for this model case resemble those realized in experiments reported in [18]. The principal differences between streamers shown in figures 5 and 8(b) are explained by the different effective sizes of spherical electrodes. Although the physical size of the spherical electrode is $b = 1 \, \text{mm}$ in both cases, the effective scaled radius bN/N_0 in figure 8(b) is smaller by a factor of two, and the effective spatial extent of the high field region in close proximity to the sphere available for formation of the streamer is reduced. As a result, the scaled radius of the formed streamer is much smaller than the one at the ground pressure (figure 5(a)). The propagation speed for this streamer is $4.5 \times 10^5 \, \text{m s}^{-1}$ and this value is between the speeds of ground and low pressure streamers shown in figure 4. In accordance with the well-known Meek condition [6, p 336] (see also the recent discussion in [27] and references cited therein), the effective distance needed for the formation of a streamer is approximately scaled as $\sim 1/N$ with the gas density and therefore in order to preserve streamer similarity one also needs to scale the gap size and radius of the sphere as $\sim 1/N$ in addition to maintaining the same reduced E/N field conditions in the discharge gap [8, 16]. Following these arguments the reduction of the effective (i.e. bN/N_0) size of the point electrode with the reduction of pressure in experiments reported in [18] should lead to the eventual suppression of streamer formation even under conditions when U/p (or E/N) parameters are kept unchanged. Indeed, it was noted in [18] that the $U = 20 \, \text{kV}$, $p = 1010 \, \text{mbar}$ case led to well developed and highly branched streamers, while streamers did not exist in the same discharge gap for a $U = 4 \, \text{kV}$, $p = 200 \, \text{mbar}$ case (i.e. with essentially the same U/p ratio). We conclude

this discussion by also noting that the non-similarity of the appearance of streamers at different pressures under conditions of the same U/p values reported in [18] generally receives contributions from both the quenching and the electrode effects discussed in this paper.

4. Conclusions

The principal results and contributions, which follow from studies presented in this paper, can be summarized as follows:

(i) We demonstrate that the quenching of singlet excited states of molecular nitrogen emitting photoionizing radiation is responsible for the non-similar behaviour of short streamers in air originating from a spherical electrode (with $1/N$ scaling of its radius) under the influence of the same reduced external electric fields at pressures higher than approximately 30 Torr. Although three-body attachment and recombination processes might contribute to the non-similar behaviour of streamers at different pressures, we can exclude contributions of these factors due to the relatively short timescales considered in the present study.

(ii) We compare our modelling results with recent experimental work on the development of positive streamers at different pressures [17, 18]. The comparison indicates that our modelling results and their interpretation based on non-similarity of the photoionization process at high pressures in air are consistent with observations, which demonstrate that streamers have more and thinner channels and branch more frequently at higher (i.e. near atmospheric) pressures than at lower pressures. We emphasize, however, that different reduced electric fields and effective (i.e. scaled as $1/N$) gap sizes and anode radii used in [17, 18] do not allow a simple separation of different physical factors affecting non-similar behaviour of streamers observed in experiments.

Acknowledgments

References

[1] Sentman D D, Wescott E M, Osborne D L, Hampton D L and Heavner M J 1995 Preliminary results from the Sprites94 campaign: red sprites *Geophys. Res. Lett.* **22** 1205–8
[2] Gerken E A and Inan U S 2005 Streamers and diffuse glow observed in upper atmospheric electrical discharges *IEEE Trans. Plasma Sci.* **33** 282–3
[3] Pasko V P, Inan U S and Bell T F 1998 Spatial structure of sprites *Geophys. Res. Lett.* **25** 2123–6
[4] Liu N and Pasko V P 2004 Effects of photoionization on propagation and branching of positive and negative streamers in sprites *J. Geophys. Res.* **109** A04301
[5] Pasko V P 2006 Theoretical modeling of sprites and jets *NATO Advanced Study Institute on Sprites, Elves and Intense Lightning Discharges* (Dordrecht: Kluwer) at press
[6] Raizer Y P 1991 *Gas Discharge Physics* (New York: Springer)
[7] Veldhuizen E M van (ed) 2000 *Electrical Discharges for Environmental Purposes: Fundamentals and Applications* (New York: Nova Science)

[8] Tardiveau P, Marode E, Agneray A and Cheaib M 2001 Pressure effects on the development of an electric discharge in non-uniform fields *J. Phys. D: Appl. Phys.* **34** 1690–6

[9] Tardiveau P and Marode E 2003 Point-to-plane discharge dynamics in the presence of dielectric droplets *J. Phys. D: Appl. Phys.* **36** 1204–11

[10] Arrayás M, Ebert U and Hundsdorfer W 2002 Spontaneous branching of anode-directed streamers between planar electrodes *Phys. Rev. Lett.* **88** 174502(R)

[11] Kulikovsky A A 2000 The role of photoionization in positive streamer dynamics *J. Phys. D: Appl. Phys.* **33** 1514–24

[12] Pancheshnyi S V, Starikovskaia S M and Starikovskii A Y 2001 Role of photoionization processes in propagation of cathode-directed streamer *J. Phys. D: Appl. Phys.* **34** 105–15

[13] Yi W J and Williams P F 2002 Experimental study of streamer in pure N_2 and N_2/O_2 mixtures and a $\approx$13 cm gap *J. Phys. D: Appl. Phys.* **35** 205–18

[14] Veldhuizen E M van, Kemps P C M and Rutgers W R 2002 Streamer branching in a short gap: The influence of the power supply *IEEE Trans. Plasma Sci.* **30** 162–3

[15] Roth R J 1995 *Industrial Plasma Engineering: vol 1. Principles* (Bristol: Institute of Physics Publishing)

[16] Achat S, Teisseyre Y and Marode E 1992 The scaling of the streamer-to-arc transition in a positive point-to-plane gap with pressure *J. Phys. D: Appl. Phys.* **25** 661–8

[17] Pancheshnyi S V, Nudnova M and Starikovskii A Y 2005 Development of a cathode-directed streamer discharge in air at different pressures: experiment and comparison with direct numerical simulation *Phys. Rev.* E **71** 016407

[18] Briels T M P, Veldhuizen E M van and Ebert U 2005 Branching of positive discharge streamers in air at varying pressures *IEEE Trans. Plasma Sci.* **33** 264–5

[19] Zheleznyak M B, Mnatsakanyan A Kh and Sizykh S V 1982 Photoionization of nitrogen and oxygen mixtures by radiation from a gas discharge *High Temp.* **20** 357–62

[20] Moss G D, Pasko V P, Liu N and Veronis G 2006 Monte Carlo model for analysis of thermal runaway electrons in streamer tips in transient luminous events and streamer zones of lightning leaders *J. Geophys. Res.* at press

[21] Babaeva N Y and Naidis G V 1997 Dynamics of positive and negative streamers in air in weak uniform electric fields *IEEE Trans. Plasma Sci.* **25** 375–9

[22] Babaeva N Y and Naidis G V 1996 Two-dimensional modeling of positive streamer dynamics in non-uniform electric fields in air *J. Phys. D: Appl. Phys.* **29** 2423–31

[23] Hockney R W and Eastwood J W 1988 *Computer Simulation Using Particles* (New York: McGraw-Hill)

[24] Press W H, Flannery B P, Teukolsky S A and Vetterling W T 1992 *Numerical Recipes in C Example Book: The Art of Scientific Computing* (Cambridge: Cambridge University Press)

[25] Cheng D K 1983 *Field and Wave Electromagnetics* (Reading, MA: Addison-Wesley)

[26] Liu N and Pasko V P 2005 Molecular nitrogen LBH band system far-UV emissions of sprite streamers *Geophys. Res. Lett.* **32** L05104

[27] Naidis G V 2005 Conditions for inception of positive corona discharges in air *J. Phys. D: Appl. Phys.* **38** 2211–14